3D FE coupled simulation of TBM tunnelling and station excavation

L. Masini[1], G. La Grotta[1], F. Lavagnini[1], and S. Rampello[1]

[1] Sapienza, University of Rome, Rome, Italy, email: luca.masini@uniroma1.it

ABSTRACT

Growing demand for mobility in major cities around the world has led to the expansion of existing underground transport networks, with the aim of alleviating congestion and promoting sustainable growth. This usually involves deep excavation and tunnelling in densely populated areas, often in close proximity to existing buildings and infrastructure. Limiting ground movement is therefore a key design priority. Further complications arise when considering the interaction between tunnelling and station excavation. This problem is usually simplified using a decoupled approach, whereby tunnel and station excavations are simulated separately to limit computational effort. The computed displacement fields are then superimposed. Conversely, coupled 3D tunnel-station numerical models can accurately reproduce the effects of the two interacting excavations, albeit at a much higher computational cost. This paper discusses aspects of the interaction between mechanised tunnelling and station excavation. The study focuses on Piazza Venezia station on Line C of the Rome Underground. A 3D finite element (FE) model has been developed to simulate the tunnelling sequences, the station excavation, and the interaction with the surrounding historic buildings. The analysis results suggest that, in the case of a very stiff excavation box, the station's stiff headwall induces a shielding effect on the propagation of tunnel-induced displacements.

Keywords: tunnelling, deep excavations, 3D FE analyses, soil-structure interaction

INTRODUCTION

The growing demand for urban mobility has led to the rapid expansion of underground transport systems, which are intended to reduce congestion and support the sustainable growth of cities. However, constructing tunnels and carrying out deep excavations in densely populated areas presents major geotechnical challenges. Such projects often take place close to existing buildings and utilities, where even minor ground movements can result in structural or serviceability issues (Mair, 2008). Consequently, controlling and minimising soil deformation during and after construction is a key design objective. Numerical modelling plays a crucial role in this process by enabling engineers to simulate soil–structure interaction (Losacco et al., 2014), predict ground responses and evaluate the effects of different construction methods. This allows design parameters to be optimised and mitigation strategies to be developed (Masini & Rampello, 2021). However, computational efforts increase dramatically when tunnel and station excavations interact, necessitating integrated modelling approaches to accurately simulate the displacement field and potential effects on nearby buildings. For this reason, simplified decoupled approaches are often adopted, whereby the displacement fields induced by tunnel and station excavations are computed separately. The resulting displacement is then obtained by superimposing the single displacement fields, using semi-empirical interaction criteria. Therefore, despite the use of advanced numerical tools, the reliability of a decoupled approach remains highly dependent on the criterion used to calculate the resultant displacement field. This is because mobilised soil nonlinearity is not explicitly considered. Consequently, the evaluation of tunnel-station interaction may not be accurate. In light of this, this paper presents the results of three-dimensional finite element (FE) numerical analyses aimed at evaluating the effects of tunnel and station excavation interaction.

The case study in question concerns Line C of the Rome Underground in the area of the future Piazza Venezia station. A 3D FE model was developed to simulate the excavation sequences of the two tunnels and the station, as well as the interaction with nearby historical buildings. Initially, analyses were conducted using a decoupled approach, simulating the different stages of excavation separately and calculating the resulting displacement field by applying the principle of superposition of effects. Subsequently, the same analyses were repeated using an integrated approach, simulating the entire excavation sequence within a single model.
Comparing the results obtained using these two approaches indicated that interaction mechanisms depend not only on nonlinear and irreversible soil behaviour, but also on the stiffness of the structural elements involved. Therefore, the results of this numerical study can be used to calibrate interaction criteria in decoupled calculation methods, thereby improving their reliability and predictive capability.

THE CASE STUDY: THE LINE C OF ROME UNDERGROUND AT PIAZZA VENEZIA

Rome's Metro Line C is the city's third underground railway line. Once fully operational, it will significantly improve connectivity between the south-eastern suburbs and the city centre, thereby alleviating traffic congestion in the urban area. The central section of the route (contracts T2 and T3) poses a significant engineering challenge due to its passage through Rome's historic centre, beneath numerous heritage buildings and valuable Roman-era archaeological sites. Contract T2, which is currently in the design stage, is particularly challenging as it extends for approximately 4 km and comprises four stations: Clodio/Mazzini, Ottaviano, San Pietro and Chiesa Nuova. Starting at Clodio/Mazzini station and heading towards Piazza Venezia, two single-track tunnels will be excavated using Earth Pressure Balance Tunnel Boring Machines (EPB-TBMs). These twin, nearly parallel tunnels will underpass the Tiber River and continue along Corso Vittorio Emanuele II, finally entering the Venezia station, which is currently under construction in Venezia Square. Several buildings of very high cultural and historical significance are located in the area where the tunnel and station excavations interact, including Palazzo Venezia, Palazzo Bonaparte, and Palazzo Doria Pamphilj.
Figure 1a shows a plan view of the area, indicating the locations of the twin tunnels and Venezia station. Figure 1b shows a schematic transverse section of Venezia station and the surrounding soils. The two running tunnels, each with a diameter of 6.7 m, are situated between 35 and 40 m below ground level. The Venezia station excavation, which is carried out using the top-down method, covers an area of 109 m × 40 m and reaches a maximum depth of 42 m. It is supported by multi-propped diaphragm walls made of cast-in-place concrete panels, which extend to around 85 m below ground level and have in-plane dimensions of 2.4 m × 1.2 m. Six permanent slabs will be installed at spacings ranging from 4.15 m to 6.4 m. A 2.5-metre-thick base slab will be cast to complete the excavation. Cross-walls will be used to control subsidence induced by the deep excavation behind the diaphragm walls. These consist of 1.2 m thick, unreinforced concrete panels arranged perpendicular to the long sides of the excavation.

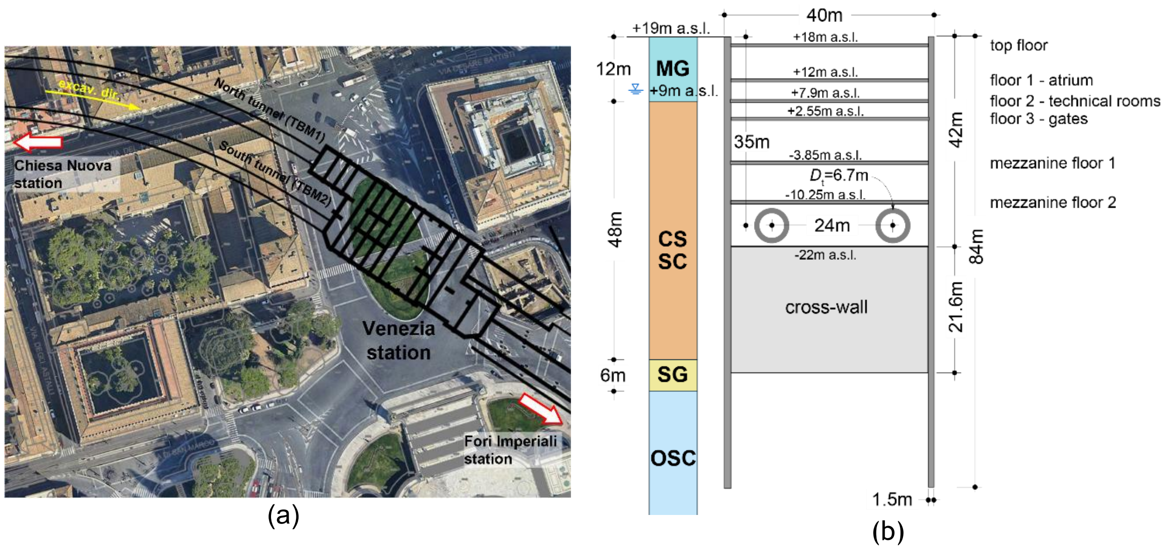

Figure 1. *Plan view of Venezia square (a). Cross-section and soil conditions (b)*

Three spacings will be used for the cross-walls: 5.3 m, 10.35 m and 15.30 m, which correspond to sets of two, three or four panels respectively. The cross-walls extend 63.6 m below ground level and 21.6 m below the formation level. Construction will proceed in two stages: (i) the erection of sacrificial buttress walls from ground level, at an elevation of 20 m above sea level (a.s.l.), and (ii) the connection of these buttresses to form continuous cross-walls from a depth of 16 m.

Soil conditions at Piazza Venezia are typical of those found in Rome's historic center (Rampello et al., 2012; Burghignoli et al., 2013). First, a 12-metre-thick layer of heterogeneous made ground (MG), mainly coarse-grained, is encountered from the nearly horizontal ground surface at +19 m a.s.l.. Underneath this are the recent alluvial deposits of the Tiber River, consisting of clayey silts and silty clays (CS-SC), extending to a depth of z = 60 m (-41 m a.s.l.) and with a thickness of about 48 m. This deposit overlies a 6-metre-thick layer of Pleistocene-age sand and gravel (SG), extending to a depth of 66 m (-47 m a.s.l.). This is followed by a thick layer of stiff, overconsolidated silty clay, known as the blue Vatican clay, which is of Pliocene age (OSC). The tunnels will be excavated in the fine-grained alluvial soils (CS-SC), while the station's diaphragm walls will be embedded in the OSC layer. Pore water pressure measurements at the site indicated that the hydraulic regime is hydrostatic, with the groundwater table located around 10 m below ground level (+9 m a.s.l.).

3D FE MODELS

Figure 2 shows the 3D FE model used to simulate the excavation of the station and twin tunnels. Analyses were carried out using the PLAXIS 3D code (Brinkgreve et al., 2013). The model represents a soil volume measuring 210 m wide, 115 m high and 176 m long. The base of the mesh is located 31 m below the toe of the diaphragm wall in the OSC soil layer. Standard fixities were applied along the mesh boundaries. The mesh consists of 577,005 10-noded tetrahedral elements with second-order interpolation on displacements. This density was chosen following a preliminary set of analyses to strike a balance between solution accuracy and reasonable calculation times.

The mechanical behaviour of the made ground (MG), sandy gravel (SG) and blue Vatican clay (OSC) layers was described using the Hardening Soil (HS) model (Schanz et al., 1999). The behaviour of the recent alluvial soil (CS-SC) was described using the HS small-strain stiffness model. This combines the HS model proposed by Schanz et al. (1999) with the elastic small-strain model developed by Benz et al. (2009). In addition to the features of the HS model, the HSsmall model can describe hysteretic soil behaviour at very small strains by introducing the initial shear modulus G_0 and the decay of the secant shear stiffness ratio G_s/G_0 with shear strain γ.

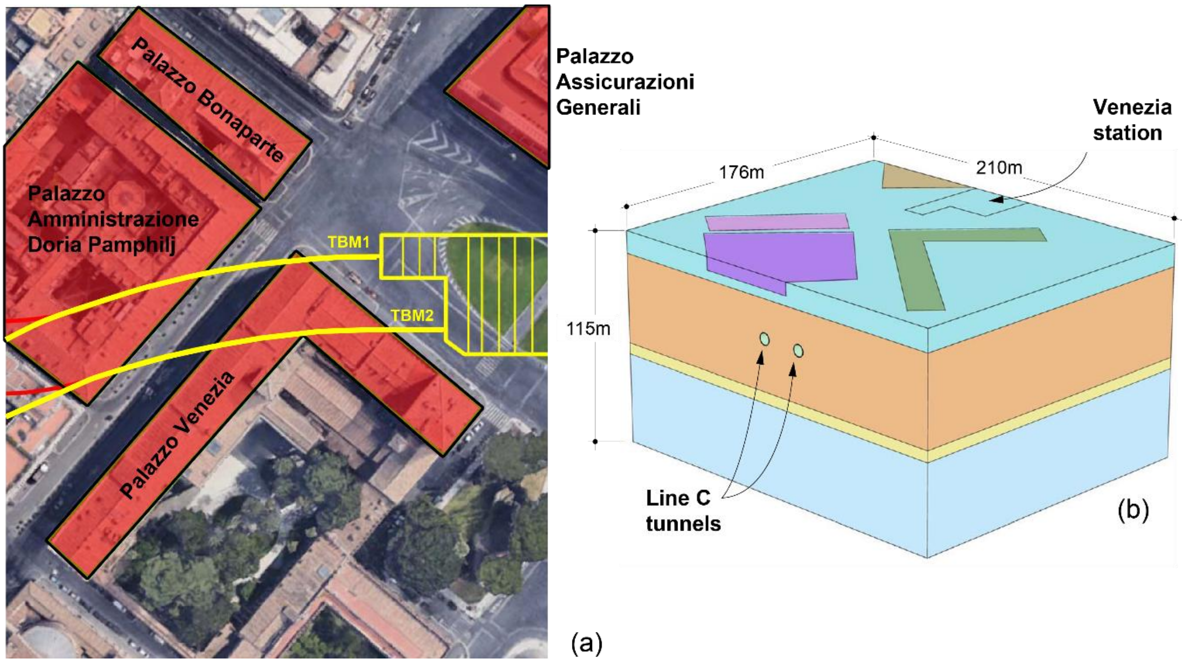

Figure 2. *Plan-view extent of the modeled area (a) and 3D finite element model (b).*

Table 1. *Soil input parameters for FE analyses*

Soil	R	CS-SC	SG	OSC
constitutive model	HS	HS small	HS	HS
γ (kN/m³)	19	18	19	20
E_{50}^{ref} (kN/m²)	26834	9367	56198	17740
E_{oed}^{ref} (kN/m²)	26834	7962	56198	17740
E_{ur}^{ref} (kN/m²)	268340	59411	561980	354790
m (-)	0.64	0.655	0.421	0.865
G_0^{ref} (kN/m²)	-	61886	-	-
$\gamma_{0.7}$	-	4.8E-04	-	-
c' (kN/m²)	5	15.4	0.1	72
φ (°)	31	26	35	25
ν	0.2	0.2	0.2	0.2
OCR (-)	2	1.2	2.5	2.5
K_0	0.485	0.608	0.426	0.85

Both constitutive models were calibrated using the results of a comprehensive geotechnical characterisation of the soils, which included field and laboratory tests (Rampello et al., 2019). Table 1 lists the input parameters adopted in the analyses.

FE analyses were performed in terms of effective stresses, with undrained behaviour assumed for the CS-SC and OSC layers and drained behaviour for the MG and SG layers due to their high-to-medium permeability. The tunnel lining was assumed to be impervious.

The calculation stages (Table 2) were defined to reproduce the main excavation activities. First, a decoupled calculation was performed using the same FE mesh, with tunnelling and station excavation simulated separately. This was followed by a coupled calculation to simulate the entire excavation sequence.

The EPBM tunnel excavation process was divided into 242 construction stages. The same steps were repeated for each stage in order to simulate support pressure at the tunnel face, the tapering shape of the TBM shield, soil excavation, installation of the tunnel lining and grouting of the gap between the soil and newly installed lining (Broere & Brinkgreve, 2002). The shaft excavation was simulated using undrained excavation stages, each of which was followed by consolidation stages lasting between 30 and 90 days.

Table 2. *FE simulation of station excavation and TBM tunnelling, calculation stages*

ID	model[a]	calculation stage
1	S, T, S+T	model initialisation (lithostatic stress state)
2	S, T, S+T	building activation (SSI analyses)
3	S, S+T	diaphragm wall activation
4	S, S+T	drained unsupported (cantilever) excavation (Δz = 7.1 m)
5	S, S+T	top floor and crosswalls activation, undrained excavation (Δz = 8.9 m)
6	S, S+T	consolidation (30 days)
7	S, S+T	floor 1 and 2 activation, undrained excavation (Δz = 1.85 m)
8	S, S+T	consolidation (30 days)
9	S, S+T	floor 3 activation, undrained excavation (Δz = 6.4 m)
10	S, S+T	consolidation (30 days)
11	S, T, S+T	TBM1 undrained passage (141 calculation phases)
12	S, T, S+T	TBM2 undrained passage (141 calculation phases)
13	S, S+T	mezzanine floor 1 activation, undrained excavation (Δz = 5.4 m)
14	S, S+T	consolidation (30 days)
15	S, S+T	mezzanine floor 2 activation, undrained excavation (Δz = 12.3 m)
16	S, S+T	consolidation (90 days)

[a] FE models: T: TBM twin-tunnel excavation only; S: station excavation only; S+T: coupled model (tunnelling + station excavation)

The 11.2 m shield, equivalent to eight tunnel rings, was modelled using 0.03 m-thick shell elements with a diameter D = 6.4 m. The following material properties were assigned: Young's modulus E = 210 GPa, Poisson's ratio ν = 0.15, and unit weight γ = 90 kN/m³. The overcutting at the rotating head and the tapering of the TBM body were modelled by applying a linear contraction to the shell elements of the shield, increasing from 0% at the head to 0.50% at the tail. This value was calibrated to achieve a volume loss V_L = 0.5% at the ground surface after the first tunnel was completed in greenfield conditions. The same contraction was adopted for TBM2 in the presence of the building. The final concrete lining, installed one ring behind the shield, was modelled as a continuous ring 0.3 m thick with an inner diameter of 6.4 m, using non-porous solid elements with a unit weight of 25 kN/m³, a Young's modulus of 30 GPa and a Poisson's ratio of 0.2. Purely frictional interface elements were used at the soil–shield and soil–lining contacts, with the angle of shearing resistance of the adjacent soil reduced by a coefficient R_{int} = 0.7. Face support pressure and pressurised backfill injection were modelled as distributed loads that increased linearly with depth. The former was applied to the soil at the face of the excavation and the latter to the intermediate zone between the shield and the permanent lining. The maximum values at the tunnel invert were 307 kPa and 357 kPa, respectively, and these values were adopted for both tunnels. These values were obtained by averaging those measured by the TBM contractor at the completed T3 stretch.

Tunnelling was modelled in discrete steps: one slice of soil (1.4 m) was removed, and the support pressure, shield and lining were advanced by an equal length from one side of the mesh to the other, resulting in a total path of 180 m.

The top-down excavation of Venezia station was simulated in twelve calculation phases to reproduce the main construction activities. The six levels of support were installed as excavation progressed. Following each undrained excavation phase, an intermediate consolidation stage of 30 days was implemented to allow for the partial dissipation of excess pore water pressure. To simulate the activation of the dewatering system that will allow the excavation to be performed safely, the piezometric level within the shaft was lowered below the current dredge level.

The diaphragm walls, supporting slabs and cross-walls supporting the deep excavation of the station were modelled using plate elements. The buildings were modelled as equivalent linear elastic solids, with a Young's modulus calibrated to reproduce the stiffness of the entire structure (Rampello et al., 2012). A uniform load was also applied to the top of each equivalent solid to simulate the weight of the building.

In the model simulating the construction of the station and tunnels, tunnelling is simulated under the assumption of undrained conditions prior to installing the final two floor slabs.

RESULTS

Figure 3 shows the contours of the vertical displacement caused by tunnelling alone. The green circles indicate the location of the second TBM. Displacements were calculated at the level of the building foundation (7 m below the ground surface) once both tunnels had been completed. In greenfield conditions, the displacement field develops almost parallel to the tunnels (Figure 3a). In contrast, compared to greenfield conditions, the weight and stiffness of the building modify the symmetry, extend the displacement field and increase the maximum settlement (Figure 3b).

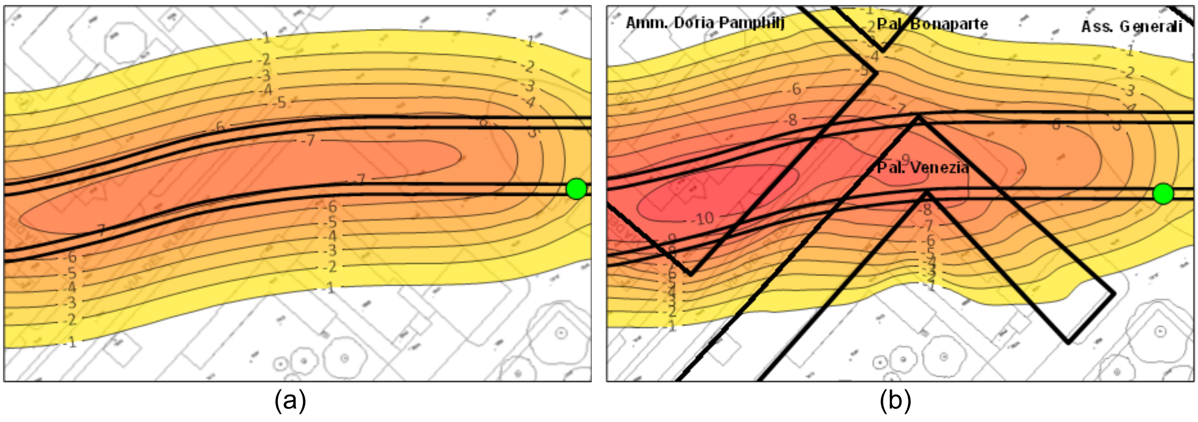

Figure 3. *Contours of the final vertical displacements (in mm) induced by tunnelling only: green-field conditions (left), with the buildings (right)*

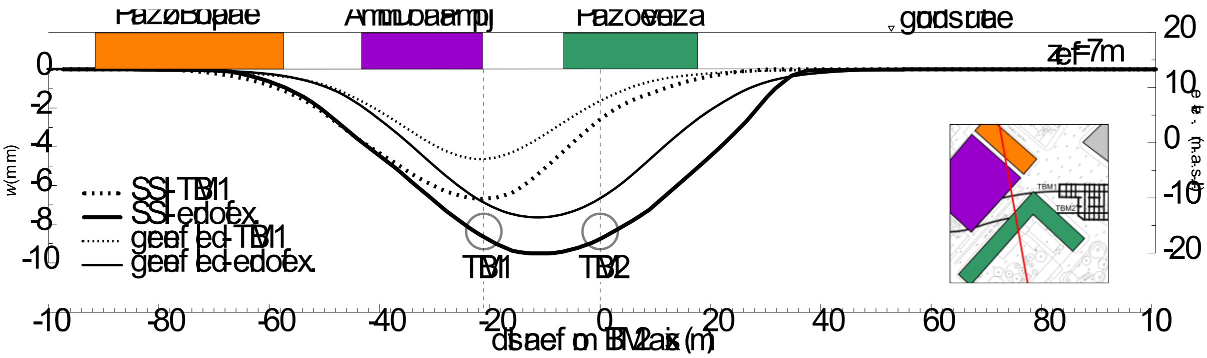

Figure 4. *Settlement troughs computed in the presence and the absence of the buildings.*

Figure 4, in particular, shows the computed transverse settlement troughs along the section marked by the red line in the same figure. The displacements induced after the passage of the first TBM are compared with those obtained at the end of tunnelling in both greenfield and built-up areas. In greenfield conditions, the passage of the first TBM, which was used to calibrate the numerical procedure adopted for simulating tunnelling, caused a volume loss of 0.5% and a maximum settlement of 4.6 mm. Once both tunnels had been completed, the volume loss had doubled to V_L = 1.04%, while the maximum settlement had increased by around 65% to w_{max} = 7.6 mm. When buildings were considered, the final volume loss and maximum settlement increased by approximately 33% (V_L = 1.38%) and 21% (w_{max} = 9.2 mm), respectively.
To emphasise the mechanisms of interaction between tunnelling and station excavation, the discussion below focuses on the results obtained under greenfield conditions. Figure 5 shows the contour lines of vertical displacement obtained from the integrated simulation of the station and tunnelling. When the first TBM is around 50 metres from the station's head diaphragm wall, the displacement fields induced by the excavation of the tunnel and shaft do not interact (Figure 5a). Excavation of the Venezia station induces a maximum settlement of 18 mm. Significant three-dimensional effects are evident, with smaller settlements developing near the short side of the station (w_{max} = 7 mm). Completing the first tunnel (Figure 5b) increases settlements mainly around the upper left corner of the station, where interaction between the two displacement fields becomes more evident. A smaller increase occurs near the head diaphragm wall, as discussed later. At the end of tunnelling (Figure 5c), the interaction effects become more pronounced, with slight extension of the resultant displacement field and an increase of approximately 3 mm in maximum settlement near the long side of the station (about +18%).

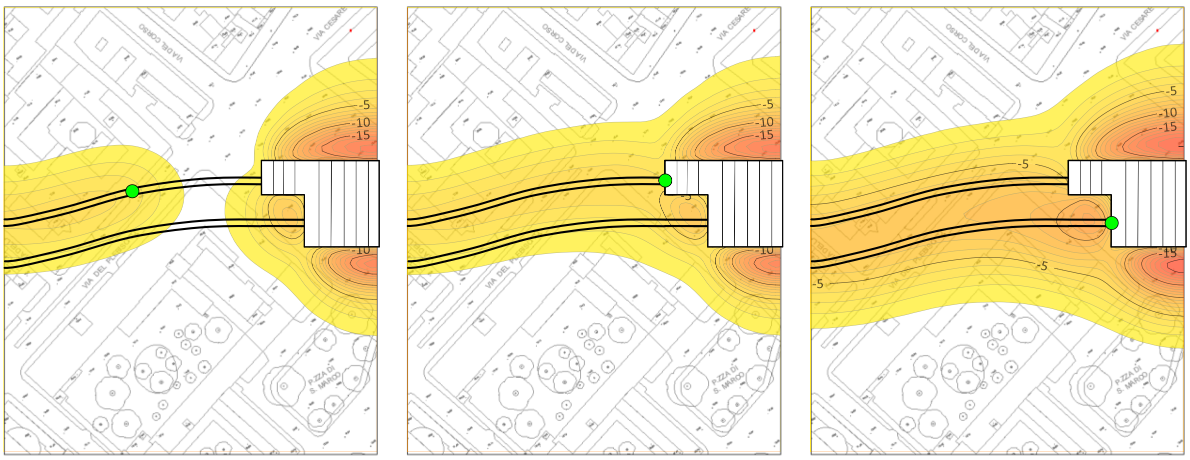

(a) (b) (c)

Figure 5. *Contours of the vertical displacements (in mm) for the coupled model, free-field conditions: TBM1 approaching the station (left), 1st tunnel completed (center) and 2nd tunnel completed (right).*

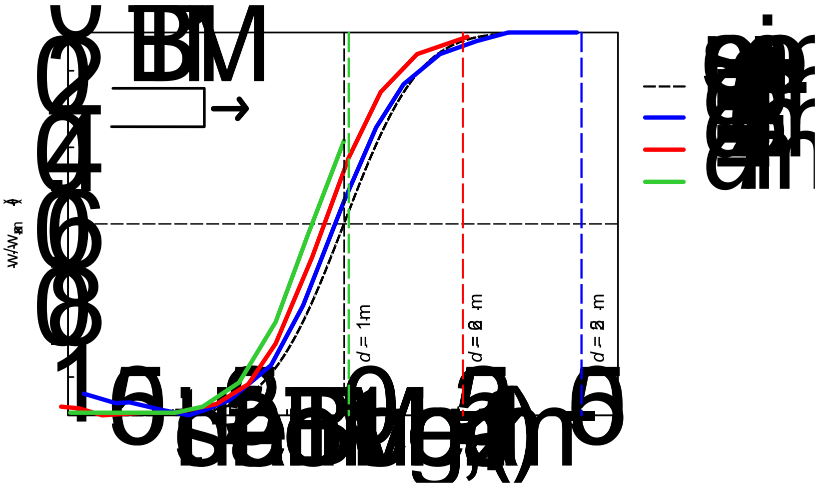

Figure 6. *Longitudinal profiles of the normalised incremental vertical displacement induced by the passage of TBM1*

Figure 6 shows the longitudinal profiles of the normalised incremental vertical displacement (w/w_{max}) induced by the passage of TBM1 plotted against distance from the tunnel face. Also included is the semi-empirical curve that predicts 50% of the maximum settlement at the tunnel face. Results are shown for three distances (d) between TBM1 and the station head diaphragm wall: 52 m, 26 m and 1 m.

The interaction between the tunnel and the station is dependent on the non-linear soil response mobilised by the preceding station excavation, as well as on the stiffness of the station's supporting structures. These effects can be evaluated by comparing settlements calculated in the presence and absence of the station. To this end, a local interaction factor has been defined at a distance x_f from the tunnel face:

$$\eta(x_f) = 1 - \frac{w_{t+s}(x_f)}{w_t(x_f)} \tag{1}$$

where $w_{t+s}(x_f)$ is the incremental settlement at distance x_f in the presence of the station and $w_t(x_f)$ is the corresponding value in its absence. The interaction factor η is equal to zero (i.e. no interaction) in the absence of the station, whereas it approaches unity when a very stiff retaining structure strongly inhibits the development of additional displacements.

When the TBM1 is far from the station (d = 52 m), the longitudinal profile remains unaffected by the deep excavation. The settlement at the tunnel face ($x_f = 0$) is 45% of the maximum value and the interaction factor is $\eta(x_f = 0) = 0$. As the TBM moves closer to the shaft, the constraining effect of the diaphragm wall reduces the displacement developing ahead of the TBM: for d = 26 m, the normalised incremental settlement at $x_f = 0$ decreases to $w/w_{max} = 0.38$, corresponding to $\eta(x_f = 0) = 0.15$. The maximum interaction effect is observed when the TBM is very close to the diaphragm wall (d = 1 m): the incremental settlement w computed at the tunnel face drops to 27% of its asymptotic value (w_{max}), with $\eta(x_f = 0) = 0.41$.

Figure 7 compares the final displacement field obtained through the decoupled approach, which superimposes the effects of tunnelling and station excavation (Figure 7a) via algebraic summation, with the displacement field computed with the coupled simulation (Figure 7b). Figure 7c emphasises the difference by showing the contour lines resulting from subtracting the displacement field of Figure 7b from that of Figure 7a. The decoupled approach notably overestimates the settlements (by approximately 20–30%) and the extent of the displacement field. However, as the settlement trough extension decreases, the gradients and, consequently, the deflections increase. These effects are concentrated near the head diaphragm wall, extending to roughly twice the width of the excavation head — that is, the short side of the excavation shaft.

Overall, although soil nonlinearity induced by the station excavation tends to increase subsequent tunnelling displacements, the stiffness of the supporting structures limits their further development. For the twin tunnels of Line C of the Rome Underground and Venezia Station, FE analyses indicate that the restraining effect of the station's supporting structures is the dominant interaction mechanism.

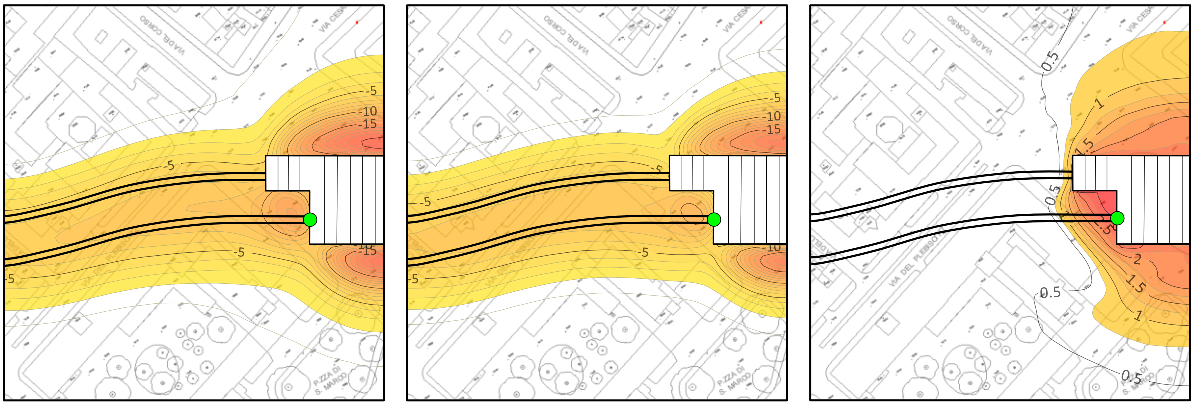

(a) (b) (c)

Figure 7. *Contours of the final vertical displacements (in mm): decoupled approach (a), coupled model (b) and difference decoupled/coupled (c).*

CONCLUSIONS

This study highlighted aspects of the three-dimensional interaction between mechanised tunnelling and station excavation. A comprehensive numerical model was developed to simulate the sequential excavation of twin EPB TBM tunnels and the top-down construction of a stiff, multi-propped station shaft in a dense urban environment, as well as the related soil–structure interaction.

Comparing decoupled and coupled simulations shows that tunnel–station interaction is governed by two competing mechanisms: (i) the nonlinear, irreversible soil response mobilised during station excavation, which increases subsequent tunnel-induced deformations; and (ii) the significant stiffness of the station retaining system, which limits displacement development as the TBM approaches the excavation. At Piazza Venezia station, the very rigid retaining structure reduced the propagation of displacements induced by tunnelling despite the large excavation depth. The head diaphragm wall provides a significant shielding effect, reducing incremental settlements ahead of the TBM by up to 40% when the machine is near the station.

The results of this study provide a basis for improving semi-empirical interaction criteria and enhancing the reliability of decoupled design methodologies for similar urban tunnelling projects, for which less computational effort is required.

REFERENCES

Benz, T., Vermeer, P.A., & Schwab, R. (2009). A small-strain overlay model. Int. Journal for Numerical and Analytical Methods in Geomechanics, 33: 25-44.

Brinkgreve, R.B.J., Engin, E., & Swolfs, W.M. (2013). Plaxis 3D user manual. Plaxis BV. Delft, The Netherlands.

Broere, W., & Brinkgreve, R.B.J. (2002). Phased simulation of a tunnel boring process in soft soil. In NUMGE 2002. Proc. of the 5th European Conference Numerical Methods in Geotechnical Engineering, Paris, France, 4-6 September 2002 (ed. P.Mestat), (pp. 529–536). Presses des Ponts.

Burghignoli, A., Callisto, L., Rampello, S., Soccodato, F.M., & Viggiani, G.M.B. (2013). The crossing of the historical centre of Rome by the new underground Line C: a study of soil structure-interaction for historical buildings. In Geotechnics and Heritage: Case Histories (Bilotta E., Flora A., Lirer S., Viggiani C. Eds.), CRC Press, London.

Losacco, N., Burghignoli, A., & Callisto, L. (2014). Uncoupled evaluation of the structural damage induced by tunnelling. Géotechnique, 64: 646–656. https://doi.org/10.1680/geot.13.P.213.

Mair, R.J. (2008). 46th Rankine Lecture: tunnelling and geotechnics: new horizons. Géotechnique, 58(9): 695–736.

Masini, L., & Rampello, S. (2021). Predicted and observed behaviour of pre-installed barriers for the mitigation of tunnelling effects. Tunnelling and Underground Space Technology, 118: 104200.

Rampello, S., Callisto, L., Viggiani, G.M.B., & Soccodato, F.M. (2012). Evaluating the effects of tunnelling on historical buildings: the example of a new subway in Rome. Geomechanics and Tunnelling, 5(3), 254-262.

Rampello, S., Fantera, L., & Masini, L. (2019). Efficiency of embedded barriers to mitigate tunnelling effects. Tunnelling and Underground Space Technology, 89: 109-124. https://doi.org/10.1016/j.tust.2019.03.027.

Schanz, T., Vermeer, P.A., & Bonnier, P.G. (1999). Hysteretic damping in a small-strain stiffness model. In NUMOG 10. Proc. of the 10th International Symposium on Numerical Models in Geomechanics, (pp 737-742). London.